Available online at www.sciencedirect.com
SCIENCE DIRECT®
Pergamon
Cement and Concrete Research 33 (2003) 1983–1997
CEMENT AND CONCRETE RESEARCH

The risk of cracking of fine hydraulic mixtures

André Lecomte[a,*], Nelly Vulcano-Greullet[a], Claude Steichen[b,1], Guy Scharfe[b,1]

[a]Département Génie Civil, Université Henri Poincaré Nancy 1, IUT de Nancy-Brabois, EA 1116 - MMGC, F-54601, Villers-lès-Nancy Cedex, France
[b]Laboratoire d'Essai des Matériaux, Ponts et Chaussées du Grand Duché de Luxembourg, 23 rue du Chemin de Fer, L-8005 Bertrange, Luxembourg

Received 23 August 2002; accepted 20 June 2003

Abstract

The hydraulic mixtures studied in this two-part article are destined for the fabrication of fine reconstituted sandstones. They were obtained from two sands whose size does not exceed 1 mm, white cement, water, and for some, from mineral additions, fibers, and superplasticizer or antishrinkage admixtures. During the elaboration, the method of fabrication created significant vertical variations in the water content, especially in the thick blocks from which were cut the $4 \times 4 \times 70$ cm test pieces used in the shrinkage measurements. The first part of the article presented in detail the materials, the formula adjustments, estimates of the rates of hydration and carbonation, and the various measurements. This second part is devoted the models retained for the description of the evolution of the characteristics of these products as well as simulation involving a likely cracking index.

Keywords: Curing; Compressive strength; Elastic moduli; Shrinkage; Modeling

1. Introduction

Let us first recall that the major dimensional variations of hydraulic materials are due to the hydration of the cement (endogenous shrinkage) and then to the desiccation of the hardened paste (drying shrinkage). It is well known that the accompanying departure of the water creates a binding phase capillary depressions, which binding phase is then submitted to strong internal compression. It is the associated shrinkage stresses that deform the composite in keeping with elasticity and creep laws and as function of the properties of the prevailing phases.

Three models used in calculating hydraulic concrete shrinkages were compared in regards to the deformations observed on the different formulas of the reconstituted sandstones [1]. The first is the model associated with BetonlabPro2 software [2,3] that especially bases the estimation of the long-term total shrinkage on the elasticity properties of the composite, which properties are in fact deduced from the formula. The other two are more empirical models of AFREM and CEB-FIB (taken from Eurocode 2 [4]), respectively, presented by Le Roy et al. [5] and Müller et al. [6]. Both models describe the evolution of the endogenous shrinkage and the desiccation as a function of the mechanical strength at 28 days, the average radius of the test pieces, and the prevailing hydric conditions of the environment.

After briefly recalling the principles of the three models, the article presents their application to the high porosity reconstituted sandstones. Eventual observed differences are then used to adjust some of the coefficients that were initially calibrated on the concretes. One then chooses the tool that is especially the most adapted for expressing a likely cracking of the materials. This index helps to class the formulas by their sensitivity to dimensional variations.

2. Concrete shrinkage models

2.1. BetonlabPro2 software associated model

The calculation of the endogenous and the total shrinkages in the BetonlabPro2 software [2] is based on the three-sphere model [7] (Fig. 1). This is a homogenization

* Corresponding author. Tel.: +33-3-83-68-25-75; fax: +33-3-83-68-25-32.
E-mail addresses: andre.lecomte@iutnb.uhp-nancy.fr (A. Lecomte), nellyvulcano@yahoo.com (N. Vulcano-Greullet), steichen@pch.etat.lu (C. Steichen), gscharfe@vo.lu (G. Scharfe).
[1] Tel.: +252-310-502-252/200; fax: +252-317-311.

0008-8846/$ – see front matter © 2003 Elsevier Ltd. All rights reserved.
doi:10.1016/S0008-8846(03)00221-7

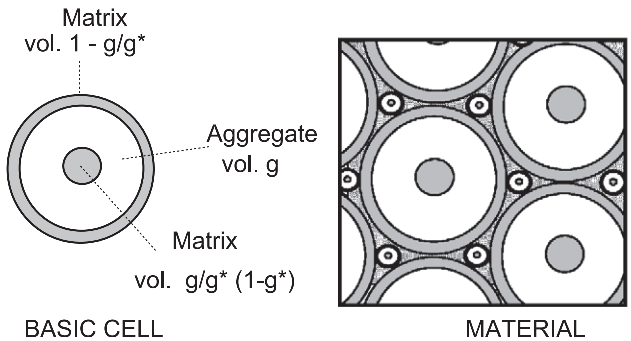

Fig. 1. The triple-sphere model [3,4,7].

model, an extension of the two-sphere model due to Hashin [8] in which a three-sphere is an elementary cell made up of three concentric spheres with the two innermost spheres representing a virtual aggregate of granular phase g at the center of part of paste (the matrix) of volume $1-g^*$ (g^* is the packing density of the tight packing of the dry grains). The external sphere is formed by the rest of the paste, which gives the concrete its workability. As the concentration of the virtual aggregate, the mixture is g/g^*, the three respective volumes per unit volume of mixture are g for the aggregate sphere, $g/g^*(1-g^*)$ for the sphere of the inner matrix and, $1-g/g^*$ that of the outer matrix.

Using the compressibility and shear moduli derived from the Hashin–Shtrikman bounds [9] and applying the equations of elasticity to the three-sphere structure under hydrostatic stress and, by extension to the entire material, and with the assumption that the Poisson coefficient of the two constituents is equal 0.2 [7], the endogenous shrinkage $\varepsilon_{\mathrm{es}}$, can be expressed by the following equation:

$$\varepsilon_{\mathrm{es}} = k\varepsilon_{\mathrm{es}}^{\mathrm{m}},$$

$$\text{with } k = \frac{\left(1+\dfrac{E_{\mathrm{md}}}{E_g}\right)\left(1-\dfrac{g}{g^*}\right) + \dfrac{4\dfrac{E_{\mathrm{md}}}{E_g}(1-g^*)\dfrac{g}{g^*}}{g^* + \dfrac{E_{\mathrm{md}}}{E_g}(2-g^*)}}{1+\dfrac{g}{g^*}+\dfrac{E_{\mathrm{md}}}{E_g}\left(1-\dfrac{g}{g^*}\right)} \tag{1}$$

$\varepsilon_{\mathrm{es}}^{\mathrm{m}}$ and E_{md} are respectively the endogenous shrinkage and the delayed modulus of the matrix (which takes into account the intrinsic creep). E_g, g, and g^* are, in the corresponding order, the aggregate modulus, real, and maximal packing densities. The g^* is generally calculated using the model compressible packing model (CPM) [3], and g is deduced from the formula of the concrete. E_g can either be measured on the original rock of the aggregate or estimated from the measurements of the concrete by calibration with the model. The matrix modulus E_{md}, which should logically be related to the strength of the paste, is in reality altered by the interactions with the aggregate. It is on the contrary well correlated to the composite compressive strength fc according to the relation:

$$E_{\mathrm{md}} = 50.6(1+0.966\psi)\mathrm{fc} \tag{2}$$

where ψ describes the relative contribution of the cement equivalent pozzolanes as in:

$$\psi = 1.1\left[1-\exp\left(-K_{\mathrm{p}}\frac{\mathrm{pz}}{\mathrm{c}}\right)\right] \tag{3}$$

K_p is a coefficient that measures the activity of the pozzolanas, and c and pz are mass dosages Portland cement (clinker) and in pozzolana, respectively.

The matrix endogenous shrinkage $\varepsilon_{\mathrm{re}}^{\mathrm{m}}$ is obtained by making reference to the concept of long-term hydric stress σ_{H} [5] and the delayed elastic modulus E_{md}:

$$\varepsilon_{\mathrm{es}}^{\mathrm{m}} = \frac{\sigma_{\mathrm{H}}}{E_{\mathrm{md}}} \text{ with } \sigma_{\mathrm{H}} = K_{\mathrm{c}}\left(0.631-\frac{\mathrm{w_f}}{\mathrm{c}}\right)(1+3.11\Psi) \tag{4}$$

K_{c} represents the influence of the cement nature on the endogenous shrinkage.

Using the three-sphere model, the BetonlabPro2 software also calculates the total long-term shrinkage $\varepsilon_{\mathrm{ts}}$ using the relation:

$$\varepsilon_{\mathrm{ts}} = \varepsilon_{\mathrm{ts}}^{g} + k(\varepsilon_{\mathrm{ts}}^{\mathrm{m}} - \varepsilon_{\mathrm{ts}}^{g}) \tag{5}$$

where $\varepsilon_{\mathrm{ts}}^{\mathrm{m}}$ and $\varepsilon_{\mathrm{ts}}^{g}$ are, respectively, eventual total shrinkages of the matrix and the aggregate, and k is as defined in Eq. (1). $\varepsilon_{\mathrm{ts}}^{\mathrm{m}}$ is related to the mortar compressive strength $\mathrm{fc_{m28}}$ and can be calculated from the composition of the concrete according to the relations given in the sequel. For 160-mm test pieces exposed after a 28-day curing in an environment of 50% relative hygrometry, $\varepsilon_{\mathrm{ts}}^{\mathrm{m}}$ is given by:

$$\varepsilon_{\mathrm{ts}}^{\mathrm{m}} = 0.0286^{\mathrm{fc}_{\mathrm{m28}}^{-0.414}} \tag{6}$$

By comparing the tensile stress created in the composite aggregate by these shrinkages to the tensile strength ft of the material, one can estimate a cracking index for the endogenous shrinkage Ic_{es} and the total shrinkage Ic_{ts}, making the assumption that all these shrinkages are avoided, as can for instance happen with sealed stones in constructions:

$$Ic_{es} = \frac{\varepsilon_{es} E_d}{ft} \quad Ic_{ts} = \frac{\varepsilon_{ts} E'_d}{ft} \tag{7}$$

E_d and E'_d are the delayed modulus of the composite, which take into account the intrinsic creep due to the endogenous shrinkage and the total creep due to the total shrinkage under dry conditions, respectively. These two moduli and the instantaneous modulus E are also calculated from the aggregate and the matrix moduli using the three-sphere model:

$$E = k_m E_m$$

$$\text{with } k_m = \left(1 + 2g \frac{E_g^2 - E_m^2}{(g^* - g)E_g^2 + 2(2 - g^*)E_g E_m + (g^* + g)E_m^2}\right) \tag{8}$$

and

$$E_d = k_{md} E_{md} \text{ and } E'_d = k'_{md} E'_{md} \tag{9}$$

The coefficients k_{md} and k'_{md} are obtained by replacing E_m in the above expression for k_m by E_{md} and E'_{md}, respectively. E_{md} is as defined earlier on. The matrix instantaneous modulus E_m and delayed modulus E'_{md} are given by the following relations:

$$E_m = 226\text{fc and } E'_{md} = 28.5(1 + 0.935\psi)\text{fc} \tag{10}$$

As the different moduli of the matrix (E_m, E_{md}, and E'_{md}) are directly associated with the compressive strength of the composite, we deem it important to recall again the corresponding model associated with the software. It is based on the composition, the characteristics, and the granular structure of the constituents. One thus first calculates the quantity of equivalent cement:

$$c_{eq}(t) = c\left[1 + 1.1\left(1 - \exp\left[-\frac{\sum K_{p,i}(t)\text{pz}_i}{c}\right]\right) + 0.017 t_{C_3A}\left(1 - \exp\left[-79\frac{\sum \text{fi}_j}{t_{C_3A} c}\right]\right)\right] \tag{11}$$

and then the matrix strength $fc_m(t)$:

$$fc_m(t) = 13.4\ \sigma' c_{28}\left[d(t) - 0.0023\frac{d(7)}{t} \times \frac{\sum S_{FI,j}\text{fi}_j}{c} + \left(1 + \rho_c\frac{w_f + a}{c_{eq}(t)}\right)^{-2.85}\right]\text{MPT}^{-0.13} \tag{12}$$

with

$$\text{MPT} = D_{max}\left(\sqrt[3]{\frac{g^*}{g}} - 1\right) \tag{13}$$

and the composite compressive strength fc_t:

$$fc_t = \frac{p\ fc_m(t)}{q\ fc_m(t) + 1} \tag{14}$$

Previously undefined terms appearing in the preceding relations are:

- $d(t)$, a kinetic parameter describing the rise in the strength of the cement,
- $d(7)$, the value of the preceding parameter at 7 days,
- w_f, free water per unit volume,
- a, air per unit volume,
- t_{C3A}, percentage of C_3A content in Portland cement (clinker),
- fi, per unit volume weight of limestone fillers of surface mass S_{FI},
- $\sigma' c_{28}$, the true class Portland cement of density ρ_c,
- MPT, the maximum thickness of the paste, represents the interval that separates two initially touching grains of size D_{max} after injection of the binding matrix into the optimized dry grain stacking,
- D_{max}, the sieve size, which allows the passage of 90% of the aggregate mixture,
- p, a coefficient of adhesion between the paste and the aggregate (bond coefficient),
- q, a coefficient of the aggregate limiting effect (ceiling coefficient).

Finally, the tensile strength ft is calculated from the compressive strength fc according to the relation:

$$\text{ft} = k_t \text{fc}^{0.57} \tag{15}$$

These models, the foundations of which are presented in Ref. [3], reproduce to a good accuracy the various shrinkages, moduli, and strengths observed on a wide variety of concretes and mortars, especially of the HPC type. However, the size of the biggest grains in these mixtures never exceeded 5 mm and the test pieces were either protected against drying or placed in curing, at least in the early age. It is therefore interesting to apply their principles to the particularly fine products of ours, some of which were exposed right after their fabrication.

2.2. AFREM model

Le Roy et al. [5] proposed a simplified model for the calculation of deformations respecting the regulations for HPC deformations especially. It was developed within the framework of the French association for research on and testing building materials, Association Française de Recherches et d'Essais sur les Matériaux de construction

(AFREM). The code was the result of shrinkage and creep observations made by Le Roy [7] on a great number of concretes or found in the literature. It is essentially based on the characteristic strength of the concrete at the compressive strength f_c before or on Day 28 (f_{c28}), the age of the concrete at the start of the drying (t_s), the average radius of the piece (r_m), and the external relative humidity (RH).

The proposed model for the endogenous shrinkage has two parts. The first concerns the shrinkage up to Day 28 and the second the shrinkage after Day 28. They are as follows:

– for $t<$ 28 days

$$f_c/f_{c28} < 0.1 \quad \varepsilon_{re}s(t,f_{c28}) = 0$$

$$f_c/f_{c28} \geq 0.1 \quad \varepsilon_{es}(t,f_{c28}) = (f_{c28}-20)\left(2.2\frac{f_c}{f_{c28}} - 0.2\right)10^{-6} \tag{16}$$

– for $t \geq 28$ days

$$\varepsilon_{es}(t,f_{c28}) = (f_{c28}-20)\left(2.8 - 1.1\exp\left(-\frac{t}{96}\right)\right)10^{-6}$$

The model for the drying shrinkage ε_{ds} is the product of several terms, which are also expressed as function of the strength at Day 28:

$$\varepsilon_{ds} = K_{ds}(h_r - RH)10^{-6}f(t) \tag{17}$$

– K_{ds} takes into account the rigidity of the concrete. Its value is given by:

$$\begin{aligned} K_{ds} &= 18 && \text{for } f_{c28} \leq 57 \text{ MPa} \\ K_{ds} &= 30 - 0.21 f_{c28} && \text{for } f_{c28} > 57 \text{ MPa} \end{aligned} \tag{18}$$

– h_r is the internal relative humidity attained through self-desiccation. It is given by the relation:

$$h_r = 72\exp(-0.046 f_{c28}) + 75 \tag{19}$$

– $f(t)$ is a kinetic function that can be written as:

$$f(t) = \frac{t-t_s}{t-t_s+br_m^2} \tag{20}$$

where b is a constant whose value is 2.8 or 8.4 depending on whether or not the concrete contains silica fumes. Remember that r_m is the average radius of the piece, in the present case, the cross sectional area divided by the perimeter (m) in contact with ambient medium.

2.3. CEB-FIP model

Exploiting the RILEM database, Müller et al. [6] proposed an extension to the CEB-FIP shrinkage model [10] to cover concretes ranging from ordinary concretes to HPC concretes. This model was retained in the Eurocode 2 [4]. The total shrinkage $\varepsilon_{cs}(t,t_s)$ of the concrete at age t and exposure at age t_s and in a medium of relative humidity RH (%) is given by some of the endogenous shrinkage $\varepsilon_{cas}(t)$ and the desiccation shrinkage $\varepsilon_{cds}(t,t_s)$ calculated, respectively, according to the relations:

$$\varepsilon_{cas}(t) = \varepsilon_{cas\ 0}(f_{c28})\beta_{as}(t) \tag{21}$$

and

$$\varepsilon_{cds}(t,t_s) = \varepsilon_{cds\ 0}(f_{c28})\beta_{RH}(RH)\beta_{ds}(t-t_s) \tag{22}$$

with:

$$-\varepsilon_{cas\ 0}(f_{c28}) = -\alpha_{as}\left(\frac{f_{c28}/f_{c0}}{6+f_{c28}/f_{c0}}\right)^{2.5}10^{-6}$$

a coefficient of endogenous shrinkage,

$$-\beta_{as}(t) = 1 - \exp\left(-0.2\left(\frac{t}{t_1}\right)^{0.5}\right)$$

a function describing the evolution of this shrinkage,

$$-\varepsilon_{cds\ 0}(f_{c28}) = [(220 + 110\alpha_{ds1})\exp(-\alpha_{ds2}f_{c28}/f_{c0})]$$

a coefficient of desiccation shrinkage,

$$-\beta_{RH}(RH) = \begin{cases} -0.25 & \text{if RH} \geq 99\%\beta_{s1} \\ -1.55.\left(1-\left(\frac{RH}{RH_0}\right)^3\right) & \text{if } 40 \leq \text{RH} < 99\%\beta_{s1}, \end{cases}$$

a coefficient that takes into account the relative humidity in the desiccation shrinkage,

$$-\beta_{ds}(t-t_s) = \left(\frac{(t-t_s)/t_1}{350(h/h_0)^2 + (t-t_s)/t_1}\right)^{0.5},$$

a kinetic function describing the evolution of this shrinkage.

Here are the values of the different coefficients used in the preceding functions:

- α_{as}, α_{ds1}, and α_{ds2} are equal to 800-700-600, 3-4-6, and 0.13-0.11-0.12, respectively, depending on whether the cement hardens slowly or fast,
- $f_{c0} = 10$ MPa,
- $t_1 = 1$ day,
- $RH_0 = 100\%$,
- $h_0 = 100$ mm,
- $h = 2A_c/u$ is the mean radius of the piece, where A_c is the area of the cross section (mm^2) and u the perimeter of the piece in contact with the external medium (mm).
- $\beta_{s1} = \left(\frac{3.5f_{c0}}{f_{c28}}\right)^{0.1} \leq 1.0$

3. Application of the BetonlabPro2 mechanical models to artificial sandstones

The strengths of the artificial sandstones were measured on certain formulas at various dates [1]. The first stage of the simulation was therefore to compare the BetonlabPro2 mechanical models to the available results. The specific parameters of the materials were determined from tests realized on 16×32 cm cylindrical test pieces, and $4 \times 4 \times 16$ prisms were kept in water at 20 °C for 28 days in keeping, with approach elaborated in Ref. [3]. Table 1 shows the values obtained. To be more explicit, for the aggregates, the coefficients p, q, kt, and its modulus E_g, and for the cements and the additions, the coefficients or functions σ'_{c28}, K_c, $d(7)$, $d(t)$, and $K_p(t)$. In the calculations presented in the sequel, the preceding parameters are weighted in proportion to the respective per unit volume dosages. We recall that the measurements of bending tensile strengths of the $4 \times 4 \times 16$ prisms were assigned a scale effect coefficient of 0.58. Similarly, the coefficient 13.4 of Eq. (12) was replaced by 11.4 to take into account the 4×4 cm^2 section of the prisms submitted to the tests [3].

Table 1
Main properties of the constituents used for the fabrication of artificial stones

Constituents		Sg	Sc	CEM I	CEM II	LF	SF
Surface mass (m^2/kg)		290		314	490	290	3400
Rate (%) of limestone fillers		5	0	4	19	100	
Rate of clinker (%)				96	81		
Bogue composition of the clinker	C_3S			61.8	61.8		
	C_2S			23.4	23.4		
	C_3A			10.9	10.9		
	C_4AF			1.3	1.3		
Compressive strength (MPa)	2*j*			26.1	30.4		
	3*j*			33.2	36.9		
	7*j*			42	39		
	28*j*			58.9	53.9		
	–	45					
Modulus of elasticity (GPa)		54	75				
Bond coefficient (p)		0.81	0.80				
Ceiling coefficient (q)		0.005	0				
Tensile coefficient (kt)		0.46	0.48				
Coefficient of endogenous shrinkage (K_c)				19	19		
Kinetic term, $d(7)$				−0.0150	−0.0116		
Kinetic function, $d(t) = a\log(t) + b$	a			0.0247	0.0189		
	b			−0.0357	−0.0272		
Coefficient of activity humid medium, $K_p(t) = \alpha\log(t) + \beta$	α						6.5
	β						−1.66
Coefficient of activity dry medium, $K_p(t) = \alpha'\log(t) + \beta'$	α'						2.57
	β'						0.08

Table 2
Parameters for calculating the strength of the matrix of each formula

Formulas	Slab	D_{max}	g	g^*	MPT
A	-l1	0.71	0.546	0.696	0.059
	-m3a1		0.557		0.054
	-t3b1		0.562		0.052
B	= m1	0.63	0.542	0.690	0.053
	= l3a1		0.552		0.049
	= t3b1		0.563		0.044
C	= m	0.80	0.600	0.691	0.039
D	= m	0.80	0.507	0.690	0.086
E	= m	0.80	0.565	0.690	0.055

3.1. Strength models

Table 2 gives for each of the formulas the values of D_{max}, g, g^*, and MPT used in the calculation of $fc_m(t)$. The graphs of Fig. 2 compare the compressive and the tensile strengths obtained to the experimental measurements realized at various dates, which is also given in Ref. [1]. The predictions for the mixtures protected against desiccation for at least 28 days are in close agreement with the reality no matter which formula is considered. The respective average errors are 4.7 and 2.9 MPa for the compressive strength and 0.4 and 0.5 MPa for the tensile strength for formulas protected for 28 or 160 days. BetonlabPro2 strength models can thus be validated for these particularly fine hydraulic mixtures. However, the predictions are too optimistic for test pieces exposed to air right from their fabrication or after 2 or 3 days of curing. For these, the mean errors are 0.8 and 12.8 MPa for the tensile and the compressive strengths, respectively. For this, we decided to modify the compressive strength model for the matrix (Eq. (12)) simply by engrafting a term T, which depends on the date of the product's exposure to the surrounding medium. For the sake of simplicity and the fact that the differences observed between the initial model and the experiment were globally constant for each type of preparation (Fig. 2), we chose as first approximation a relation that reduced the strength of the matrix by a uniform value ΔT no matter the age of the product. Referring to Eq. (12), the loss in strength of the matrix is given by:

$$\Delta fc_m(t) = 11.4\sigma' c_{28} \lambda \frac{\Delta T}{T} \mathrm{MPT}^{-0.13}. \qquad (23)$$

λ is a constant that depends on the nature of the cement.
By definition:

$$\Delta fc_m(28) = 0. \qquad (24)$$

The governing relation then takes the form:

$$\lambda \frac{\Delta T}{T} = \lambda \frac{28 - T}{28^* T}, \qquad (25)$$

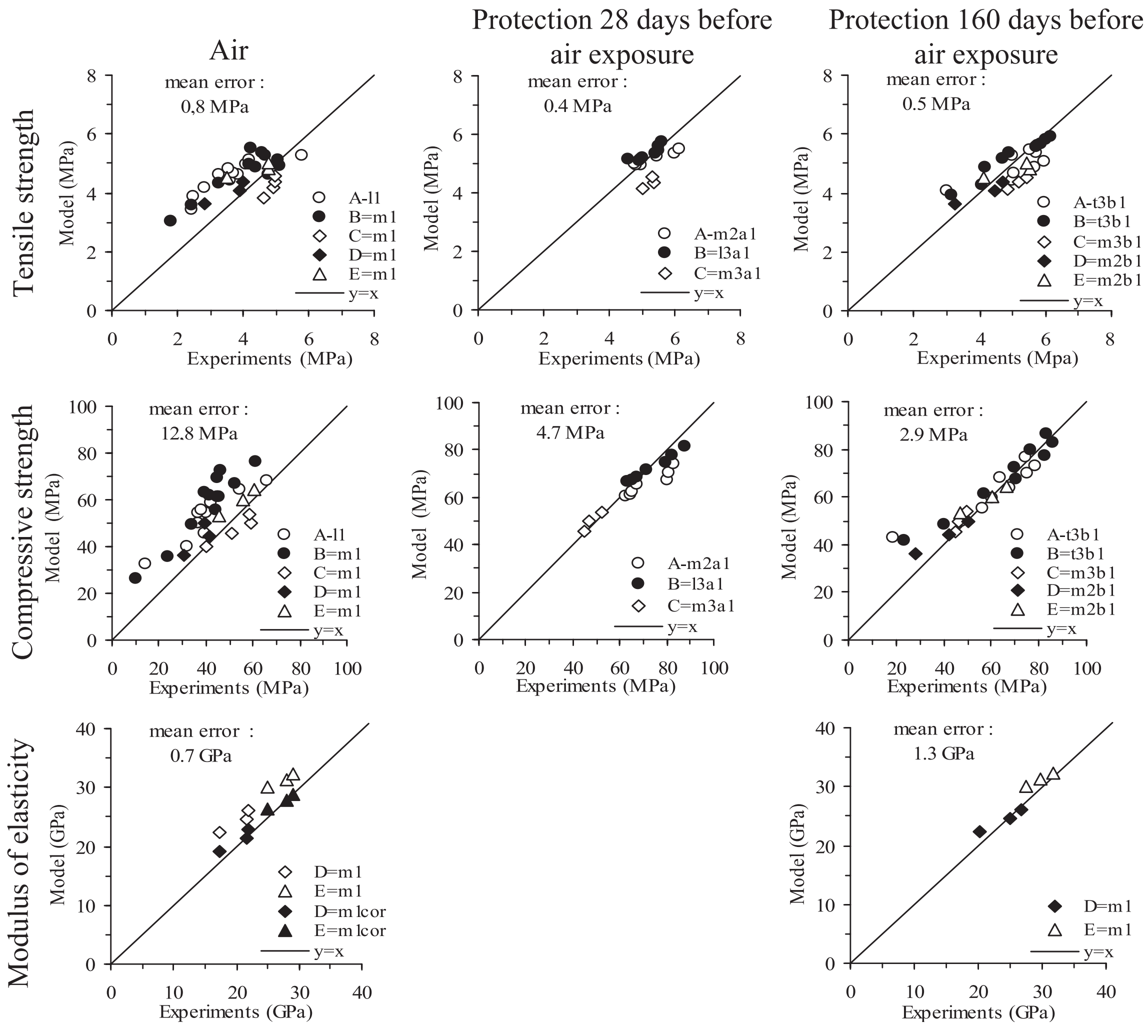

Fig. 2. Comparison between measured mechanical properties and simulation results using the initial version of the BetonlabPro2 model.

from which follows $fc_m(t)$:

$$fc_m(t) = 11.4\sigma' c_{28}\left[d(t) + \lambda\frac{28-T}{28*T} - 0.0023\frac{d(7)}{t}\frac{\sum S_{FI,j}fi_j}{c} + \left(1+\rho_c\frac{w_f+a}{c_{eq}(t)}\right)^{-2.85}\right]MPT^{-0.13} \quad (26)$$

The experimental values for ΔT were found through numerical optimization to obtain the minimum of the absolute deviation between the simulations and the results of the tests on the test pieces exposed to air from their fabrication (Formulas A and B) or after 2 days (Formula E) or 3 days (Formula D) of conservation under water. The Formula C was excluded from this adjustment because of the presence of fibers. The results are presented in Fig. 3a, which shows a good agreement between the experiment and the smoothing. The constant λ is equal to the value of ΔT at $T=1$; in the present case, $\Delta T = -0.0244$ for the two cements made from the same clinker. It can be observed that the negative effect on the strength sharply diminishes if the test pieces are protected for at least 4–6 days. On the contrary, there is a slight improvement in the strength of test pieces protected for more than 28 days compared to that of test pieces exposed to air on Day 28. For the unprotected test pieces, the application of the modified model leads to a mean error comparable to that of the other tests, namely, 0.4 MPa for the tensile strength (Fig. 3b) and 3.9 MPa for the compressive strength (Fig. 3c).

Finally, in regards to Formula B, which contains silica fume, it is to be noted that its activity coefficient $K_p(t)$ was not measured on ISO mortars but fitted from the results of test pieces of artificial stones (which in fact mortars) protected against desiccation for 28 or 160 days. The corresponding values represented by a straight line in a semilogarithmic coordinate system (coefficients α and β given in Table 1) are very high on account of very high long-term strengths obtained. Thus, for instance, the term $K_p(28)$ takes the exceptional value 7.7 (value published in the existing literature do not exceed 6). This can be explained by the very pure nature of the white silica fumes (content in SiO_2>98%) used here in a nondensified

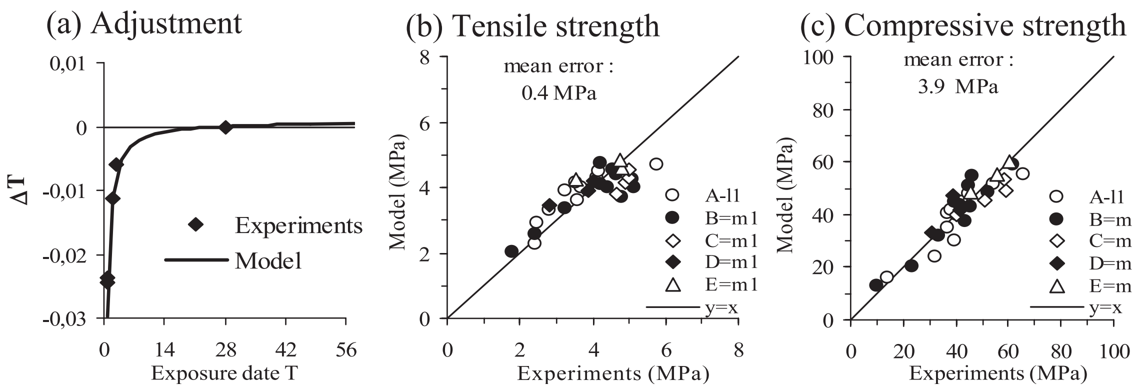

Fig. 3. Taking into account the age at which test pieces were exposed to air and new comparison between the mechanical properties and the results of experimental simulation using BetonlabPro2 modified models.

form. But the activity of this addition must be reduced significantly before one can obtain the performances of test pieces of this same formula that were, on the contrary, exposed to air only a day after their fabrication. It is therefore justified to think that premature depart of water also reduces the pozzolana activity of this addition. The best fitting was obtained when the coefficients α' and β' were equal to 2.57 and 0.08, respectively (Table 1). In this case, the value of $K_p(28)$ is only 3.8.

Modified in this manner, the BetonlabPro2 strength models are appropriate for these fine hydraulic products, no matter the formula and the age of exposure to air. However, it would require other measures before the proposed modifications could be generalized to commonly used concretes, the formworks of which are removed on construction sites just a day after their preparation and which are known to suffer a substantial drop in strength compared to products that have been protected for a longer period of time [11]. These measures would allow the integration of the nature of the cement and the average radius of the pieces into the coefficient λ.

3.2. Elasticity models

The next stage of the modeling consisted in calculating the moduli of elasticity E for the different products (Eqs. (8) and (9)) and to compare them (Fig. 2) to those measured on test pieces of the Series D and E [1]. Here again, we found a good agreement of the results for the pieces, which were under water for 160 days (mean error of 1.3 GPa) thereby validating the BetonlabPro2 elasticity models for these fine products. Once again, the test pieces exposed to immediately after their fabrication (transparent points on Fig. 2) show a significant difference (a mean error of 4.1 GPa). In principle, these differences should not have existed since the calculation of the elasticity moduli E took into consideration the already penalized compressive strength on account of the negative effect of the premature exposure to air (Eq. (26)). It seems then that the elastic properties of these products suffer additional modifications probably linked with the importance of the shrinkage (and creep) that occurs at the young age and which can provoke a substantial internal shrinkage restrained, especially in the corona of transition. Unfortunately, the scantiness of available measurements excluded any attempt at parameterization. As first approximation and only for these products, we simply adjusted the coefficients linking E_m to fc (Eq. (10)) so as to minimize the difference between the model and the experiment. With a coefficient of 185 in place of the initial value of 220, the mean error was only 0.75 GPa (opaque points on Fig. 2). The coefficients linking E_{md} and E'_{md} to fc (Eqs. (2) and (10)) were also reduced in the same proportion, respectively, giving 43.0 and 24.2, instead of the initial values of 50.6 and 28.5.

3.3. Conclusion

We retain from these calculations that BetonlabPro2 mechanical models, initially validated on concretes, are also appropriate for much finer hydraulic products. The methods underlying these tools, which consider the characteristics of the binder and the additions, the aggregates (p, q, and kt, E_g...), and the granular structure (g, g^*), thus appear to be valid no matter the size of the grains. Only few adaptations were needed to take into account the low performances of test pieces that were prematurely exposed to air. We thus obtained, to a reasonable accuracy, the same set of measurements realized on the different formulas of the artificial sandstones for various values of the ratios w/c and for the different conditions of conservation. The mechanical properties needed for the coming modeling of deformations will therefore be supplied by these tools.

4. Fine artificial sandstone shrinkage modeling

4.1. BetonlabPro2 software associated models

BetonlabPro2 shrinkage models give only the long-term deformations, which are generally sufficient for establishing comparisons between formulas (see further on in the sequel). The shrinkages are calculated using the three-sphere model and from the aggregate modulus, the matrix delayed modulus (in cure or dry conditions), and from the shrinkage of the matrix (in cure or dry conditions) and even from the shrinkage of the aggregate (Eqs. (1) and (5)). For the endogenous shrinkage, the shrinkage of the matrix is related to the mortar compressive strength on Day 28 (Eq. (6)). In the present case, the strength was taken to be equal to that of the gravel-free artificial sandstone. The BetonlabPro2 total shrinkage model was calibrated on concrete test pieces of 160 mm in diameter kept under a condition of relative humidity of 50% after a 28-day curing under water or in a watertight envelope. Our test pieces were kept in a room regulated at the same relative humidity of 50% and some were protected against desiccation for 28 days or more. The smallness of their cross section is not a priori an inconvenience since the cross section intervenes only in the shrinkage kinetics but not in its final amplitude. Moreover, the duration of the measurements was sufficient to take it that the quasi totality of the shrinkage had been reached, putting aside the problem of carbonation [1]. The desiccation shrinkage of the rock from which the sandstone sand Sg was obtained is of the order of 170 10^{-6} [1]. This was taken into account in calculating the shrinkage of the artificial stones, in the same proportion as the per unit volume dosage of this sand in the mixture and weighting with a coefficient of 0.3 representing the percentage of grains of the same texture as the original rock and of size greater than 400 μm. The results of the calculations (simulation at the age of 1000 days) are presented in Table 3 and on the graphs of Fig. 3 (big rhombuses on the right sides of the diagrams). These plots also show the results of the experimental measurements given in part I (small rhombuses).

Once again, one sees that the predictions of the BetonlabPro2 models are relevant for the test pieces protected against desiccation for 28 or 160 days, both for the endogenous shrinkage (transparent rhombuses) and the total shrinkage (opaque rhombuses). Between the calculation and the extrapolation of the measurements to 1000 days, the mean error is only 80 10^{-6} for the long-term total shrinkages of Formulas A and B. The predictions are, on the contrary, too optimistic for the test pieces exposed to air immediately after their fabrication (mean error for all the formulas is 200 10^{-6}), probably because the pieces were not cured. Moreover, the observed shrinkages integrate extra deformations attributed to the carbonation reaction and the loss of part of the water due to this reaction [1]. For these products, we proposed a simple modification of the coefficient in Eq. (6), linking the total shrinkage of the matrix to the compressive strength of the mortar at Day 28. A good fitting is obtained with the value 0.0383 instead of the initial value 0.02286. This leads to a mean error of 40 10^{-6}. The corresponding total shrinkages are presented in Table 3 (column Modifications/air) and on Fig. 4 (modified models, second column, big rhombuses).

The shrinkages measured on Series C and D were excluded from these calculations on account of the presence of fibers (F) or of antishrinkage admixture (AS). One can now assess the effectiveness of these products by comparing the total shrinkages calculated with the model to those of the long-term measurements/extrapolations. In the case of fibers (Formula C), the shrinkage calculated for the test pieces kept in cure using the initial model and the one calculated for the pieces exposed to air using the modified model are close to the measured shrinkage (Fig. 4). Thus, propylene polymer fibers do not have a significant effect on the amplitude of the shrinkage. They, on the contrary, affect the shrinkage distribution as previously pointed out [1]. Notice that this is the formula that contains the smallest dosage in cement content and presents the least theoretical shrinkage in absolute value. In the case of antishrinkage

Table 3
Recalling a few parameters for the formulas and for calculating the delayed moduli, the endogenous and desiccation shrinkages, and the cracking indexes at Day 1000 using the BetonlabPro2 software

Formulas				Properties						
Reference	c	w_f/c	Cure (d)	E_d^a (GPa)	E'_d (GPa)	ε_{es} (10^{-6})	ε_{ts} (10^{-6})			I_{fts}
							Initial	Modifications/air	Modifications/AS	
A-l1	559	0.48	1		9.2	−163	−990	−1312		2.41
A-m3a1	571	0.44	28	16.0		−139	−866			2.39
A-t3b1	576	0.43	160	18.2		−142	−835			2.58
B=m1	541	0.45	1		10.9	−296	−1068	−1408		3.01
B=l3a1	551	0.42	28	15.9		−316	−1047			2.79
B=t3b1	563	0.38	160	18.0		−339	−983			2.87
C=m1	450	0.55	13		12.8	−58	−690	−906		2.34
C=m3a1			41	16.6		−52	−725			2.43
C=m3b1			172	17.9		−52	−724			2.61
D=m1	575	0.50	3		7.1	−175	−1202	−1593	−1012	1.51
D=m2a			160	11.5		−148	−1212		−632	1.50
E=m1	589	0.40	2		11.0	−199	−821	−1079		2.25
E=m2a			160	16.8		−171	−844			2.62

[a] At the end of the cure.

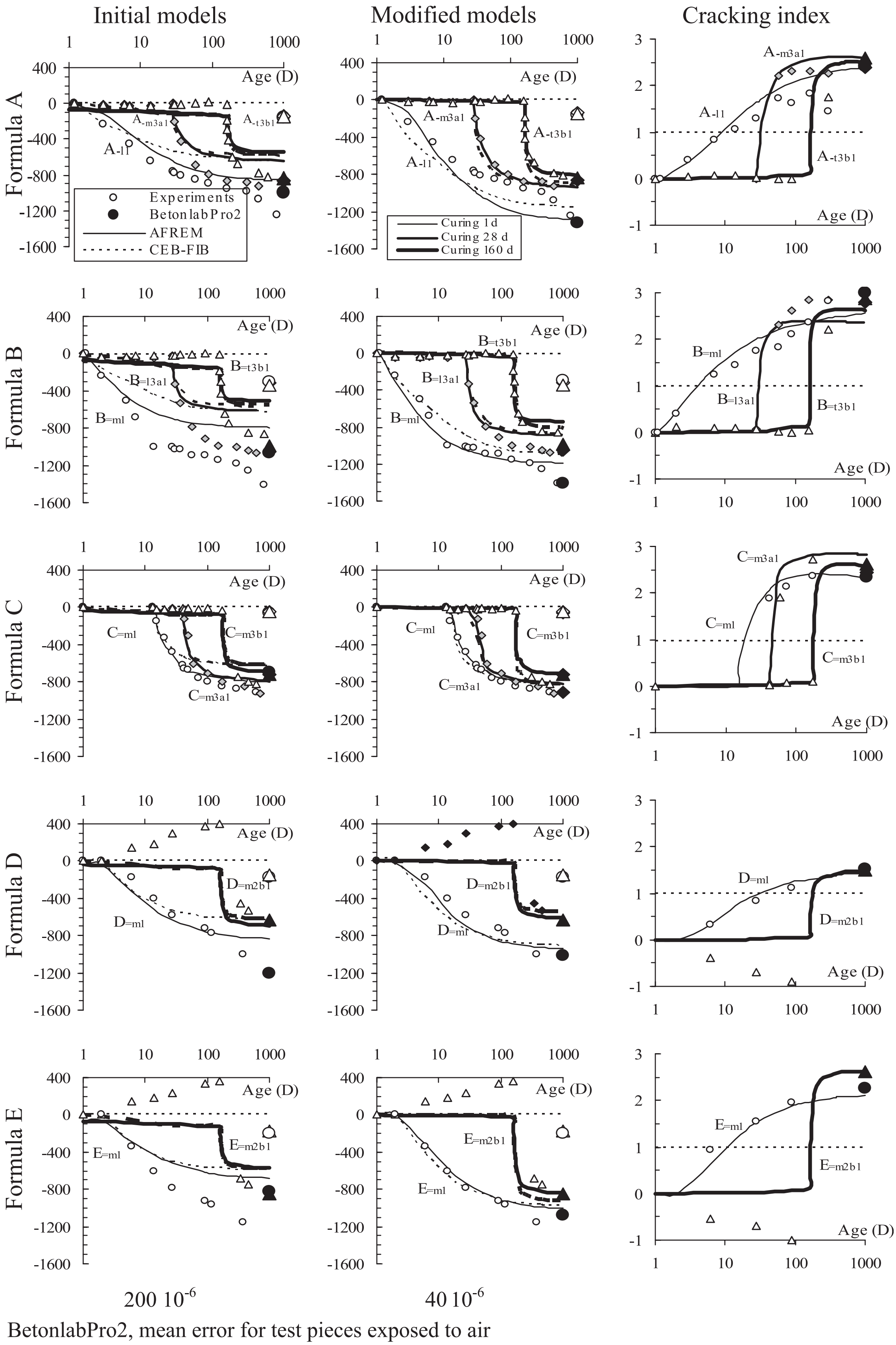

Fig. 4. Measured shrinkage [1] and modeling according to BetonlabPro2, CIB-FIB, and AFREM.

(Formula D), the model yields the highest total shrinkage ($1600\ 10^{-6}$ for the formulas that were not protected immediately after their fabrication and $1200\ 10^{-6}$ for the protected test pieces; Table 3) on account of the residual water of the mixture. The measurements effectively show a sizeable shrinkage ($1000\ 10^{-6}$ and $600\ 10^{-6}$, respectively [1]) but still lower than the theoretical value. The effectiveness of the antishrinkage for the recommended dosage used can then be expressed as the ratio of the 1000-day extrapolated value of the shrinkage measured to the value calculated at the same date. That gives $[(1600-1000)/1600] \approx 0.375$ and $[(1200-600)/1200] \approx 0.50$, respectively, for the unprotected test pieces and those hardened under cure. This product is therefore more effective when the mixtures harden under cure. BetonlabPro2 total shrinkage models were therefore assigned a reductive coefficient of 0.625 or 0.50, depending on the mode of conservation. The corresponding modified theoretical shrinkages are reported in Table 3 (Modifications/AS column) and on Fig. 4 (modified models, Formula D, big rhombuses). The coefficients are recalled in Table 5.

4.2. CEB-FIB model

The results of the simulations realized according to the CEB-FIB model are plotted in Fig. 4 (dotted curves for the initial models). For these calculations, the coefficients α_{as} for endogenous shrinkage, and α_{ds1} and α_{ds2} were taken to equal 700, 4, and 0.11, respectively, on account of the normal hardening of the cements used. The compressive strength f_{c28} at Day 28 is the one given by the modified BetonlabPro2 strength model that, it should be remembered, yields values that are very close to the experimental measurements. The other parameters involved in the desiccation shrinkage [$\beta_{RH}(RH)$ and $\beta_{ds}(t-t_s)$] depend on the rate of relative humidity prevailing during the tests (RH = 50%) and the mean radius of the test pieces. For these hydraulic products, it can be observed that whatever their formula and mode of conservation, the endogenous shrinkage predicted by this model is always higher than those measured, while the predicted total shrinkages are always lower than those measured. It is clear that this model is not really adapted to these fine hydraulic mixtures, the deformations of which are obviously more important than those of the ordinary and high-performance concretes described by the BetonlabPro2 strength model.

Our desire, however, is to have to dispose of a tool that completes the BetonlabPro2 strength model and with which to follow the time evolution of the shrinkages and determine a chronological cracking index. To this end, we adjusted two coefficients of our experimental measurements.

The coefficient α_{as} was first modified by minimizing the differences between the calculations and the measurements, realized up to Day 160, on those of test pieces of the Series A, B, and C, which were protected against desiccation during 160 days. The value 75 obtained, instead of the initial value 700, expresses the very small endogenous shrinkage that characterizes these products (incidentally, it is supposed that this shrinkage did not show in significant way before 24 h, especially for Formulas A and B).

In the second stage, only the coefficient α_{ds1} of the desiccation shrinkage model was adjusted following a similar approach, but this time by minimizing the differences between the calculations and the measurements on the test pieces of the Series A and B, which were hardened unexposed to air during 28 days. The resulting coefficient was 10 instead of 4 initially. The new values differ radically from the initial coefficients; the reasons for this can be attributed solely to the nature of the cement. The granular structure of these fine mixtures, close to a stack, plays a decisive role. It was not unfortunately taken into account in this model.

The shrinkages are plotted on Fig. 4 (dotted curves, modified models), where one can see the good final agreement with the experimental measurements, Formula D, which contains an antishrinkage, included. As in the preceding case, the shrinkage of this formula was assigned a reductive coefficient, 0.80 for mixtures prematurely exposed to air and 0.675 for those kept in cure for 28 or 160 days, to take into account the effectiveness of the this product. On the contrary, the calculated shrinkages for the Formula C are higher than those measured, probably because the w_f/c ratio is much higher than that of the other formulas. This marks the limits of the proposed adjustments for this empirical model, which are obviously valid only for formulas that to those used for the adjustments. A coefficient of 0.75 was applied to the predictions of the model to obtain the shrinkages measured on the fiber-loaded test pieces.

4.3. AFREM model

The strength characteristic f_{c28} used in the AFREM model is the average strength determined by the BetonlabPro2 mechanical model after a 15% reduction. The initial predictions obtained are slightly better than with those obtained the CEB-FIB model, with the endogenous shrinkages lower and the total shrinkages higher for all the formulas (full line curves in Fig. 4, initial models). But they are still too far from the experimental measurements to allow a direct determination of a plausible chronological cracking index.

As with the preceding case and for the same reasons (calibration of the model on concrete), certain coefficients in the initial relations were adjusted by successively minimizing the differences between the measurements up to 160 days on the test pieces A, B, and C protected for 160 days and the calculated endogenous shrinkages and then on those test pieces of A and B that were exposed to air from Day 28 and beyond (the total shrinkages).

The modified model most appropriate for these products can then be written for the endogenous shrinkage as:

- for $t < 28$ days

$$f_c/f_{c28} \geq 0.1 \qquad \varepsilon_{re}(t, f_{c28}) = (f_{c28} - 20) \times \left(0.28\frac{f_c}{f_{c28}} - 0.2\right)10^{-6}$$

- for $t \geq 28$ days

$$\varepsilon_{re}(t, f^{c28}) = (f_{c28} - 20)\left(0.9 - 1.1\exp\left(-\frac{t}{96}\right)\right)10^{-6} \quad (27)$$

For the total shrinkage, only the relation describing the rigidity of the material was modified. The appropriate relation is given by:

$$K_{ds} = 43.3 - 0.21 f_{c28} \quad \text{for } f_{c28} > 57 \text{ MPa} \quad (28)$$

As the curves for the modified model in Fig. 4 show, these modifications lead to better matching predictions with the measurements. In this case too, the calculated shrinkages for the Series C (fibered) were assigned the same coefficients as with the CEB-FIB model to take into account the presence of the fiber or the effectiveness of these products. The coefficients are reported in Table 5.

4.4. Conclusion

Of the three models tested, only that of the BetonlabPro2, essentially based on the principles of homogenization, provided relevant predictions for the fine hydraulic products investigated, be it the endogenous or the total shrinkage. It therefore constitutes a privileged tool for the determination of formulas that are less prone to cracking. Unfortunately, it only provides long-term values. This is why we modified some of the coefficients of the CEB-FIB and AFREM models so as to follow the evolution of the shrinkage and derive a time-dependent cracking index. The models modified in this way cannot be generalized to other fine products whose granular structures and nature are different, w_f/c ratios far apart, containing particular mineral additions, etc., since the corresponding effects (g, g^*, hydric constraints, the activity index, etc.) on the mechanical performances and on the shrinkage are not really taken into account in these tools. We recall that they rely only on the knowledge of the (often measured) compressive strength at Day 28 and on coefficients and functions (kinetic functions in particular) that are calibrated on concretes for they are effectively well adapted. Finally, it is to be noted that the action of the antishrinkage admixture is more interesting if the mixtures are kept in cure for a sufficiently long period of time.

5. Cracking index

This index was calculated, with respect to time, according to Eq. (7) by comparing the internal stress created by these shrinkages to the tensile strength of the materials. For products exposed to air after 28 or 160 days of curing, the cracking index for the days following the exposure to air is, however, underestimated since a delayed modulus under curing condition is higher than one calculated under dry conditions. For this reason, we simply kept the value of the delayed modulus calculated at the end of the curing condition to determine the cracking indexes between the date of exposure to air and the long term (Table 3). These moduli are provided by the BetonlabPro2 model (Eq. (9)). The shrinkages at the different dates were calculated with the AFREM model according to the prescription presented earlier on. The time-dependent tensile strengths were provided by the BetonlabPro2 mechanical model (Eq. (15)). The results are reported in Table 4 (Ic_{ts}) and the graphs on Fig. 4 (curves), where one can also read the experimental cracking indexes (symbolized by points) obtained by comparing the measured deformation combined with the appropriate modulus to the tensile strength measured at the same date (Ic_{exp}). Table 5 reports the coefficients adopted to take into account the effectiveness of fibers and the antishrinkage.

We recall that this index expresses the probability of cracking under conditions of inhibited shrinkage. An index that exceeds the critical value of 1 means that desiccation shrinkage-related cracks can appear on the skin of products common cross section and even ruptures in the case of finer pieces sealed inside a construction.

It can be seen from Fig. 4 that as long as the stones are protected, there is no risk of cracking since the endogenous shrinkage is very small. But once the stones are exposed to air, the cracking index increases rapidly to exceed the critical value only after a few days of drying. For the test pieces A, B, C, and E, which were exposed to air immediately after their fabrication, the critical value is attained after 9, 4, 5, and 12 days, respectively. For those that were protected for 28 or 160 days before exposure, the critical value is attained only after 2–5 days. In the long term, this index increases with time excepting the Formula B, which contains silica fumes. Thus, for Formulas A, C, and E, this takes 23, 2.4, and 2.6 days depending on whether the test pieces were exposed to air at an early age on Days 28 or 160. For Formula B, the respective values are 3.0, 2.8, and 2.9 days. These behaviors relate to the evolutions of the delayed moduli E_d and E'_d, which are less when the artificial stones are exposed to air at a young age. The stones are then less "fragile" in spite of their weaker tensile strength. Moreover, these indices are of the same order of magnitude as those known for concretes [2] thus showing that the fine character of the mixtures does not increase their sensitivity to this risk.

The results are different for the Formula D, which contains the antishrinkage. The critical cracking index is attained after 15 or 30 days of drying, the former for test pieces exposed to air after 160 days of curing and the latter

Table 4
Experimental and theoretical cracking indexes (deduced from the AFREM model)

	Age	Ic_{exp}	Ic_{ts}	Age	Ic_{exp}	Ic_{ts}	Age	Ic_{exp}	Ic_{ts}	Age	Ic_{exp}	Ic_{ts}	Age	Ic_{exp}	Ic_{ts}
	A-l1			B = m1			C = m1			D = m1			E = m1		
Air	1	0	0	1	0	0	36	1.87	1.98	6	0.32	0.32	6	0.93	0.83
	3	0.36	0.41	2	0.40	0.45	75	2.13	2.31	28	0.83	0.97	28	1.59	1.51
	7	0.83	0.83	7	1.25	1.36	167	2.37	2.41	90	1.11	1.24	90	1.96	1.88
	14	1.06	1.26	14	1.44	1.73									
	28	1.29	1.64	28	1.76	2.00									
	60	1.72	1.94	60	1.83	2.20									
	90	1.63	2.06	90	2.10	2.28									
	160	1.82	2.19	150	2.36	2.37									
	300	1.44	2.29	300	2.81	2.46									
	A-m3a1			B = l3a1			C = m3a1								
Protection 28 days	28	0	0	28	0	0	36	0.06	0.02						
	60	2.21	2.24	60	2.30	2.31	75	1.91	2.49						
	90	2.31	2.45	90	2.61	2.38	150	2.37	2.81						
	160	2.32	2.57	150	2.85	2.40									
	300	2.27	2.64	300	2.85	2.40									
	A-t3b1			B = t3b1			C = m3b1			D = m2b1			E = m2b1		
Protection 160 days then air exposure	1	0	0	1	0	0	36	0.03	0.02	6	− 0.4	0	6	− 0.5	0
	3	0.05	0	2	0.11	0.01	75	0.07	0.05	28	− 0.7	0.01	28	− 0.7	0.01
	7	0.08	0.01	7	0.09	0.01	150	0.09	0.08	90	− 0.9	0.04	90	− 1.0	0.08
	14	0.08	0.01	14	0.10	0.02									
	28	0.01	0.01	28	0.06	0.02									
	60	0	0.06	60	0.01	0.07									
	90	0	0.08	90	0	0.11									
	300	2.42	2.41	300	2.84	2.61									

for those exposed right after their fabrication. In the long term, the index is only 1.5. It is its lower delayed modulus combined with a higher w/c ratio that minimizes the fragility of this product whose total shrinkage, compared to other stones, remains limited (small) on account of the action of the admixture.

In conclusion, it was found that the risk of cracking for these artificial stones does not increase with if they are exposed to air right after their fabrication. It is even delayed and its long-term value is smaller (excepting mixtures incorporating silica fumes). But if the mixtures do not contain antishrinkage admixture, every stone that is totally sealed in a casing can present damaging skin cracks only after a few days period of drying. The use of propylene polymer fibers is a good way of spreading out and finally limiting these surface cracks.

Table 5
Coefficients taken into account in the effectiveness of the fibres and the antishrinkage in the models

	BetonlabPro2		CEB-FIB and AFREM	
	Fibers	Antishrinkage	Fibers	Antishrinkage
Conservation in air	1	0.625	0.75	0.80
Conservation in cure	1	0.50	0.75	0.675

6. Simulations

The calibration and the validation of the preceding models with these fine products now provide the possibility of assessing the repercussions of the variation of the terms of the formula and the mode of conservation on the properties of these artificial stones. Not only is it possible to determine the porosity and the final rate of carbonation [1], but also the mechanical performances and the shrinkage, which controls the durability of the pieces, through the cracking index Ic_{ts}.

In the simulations that follow, only the index determined from models associated with the BetonlabPro2 is considered, given the limited character of the adjustments made on the other codes of calculation. For the three modes of conservation, we first choose to assess the influence of the cement dosage, water dosage, and granular proportions on the compressive strength, total shrinkage, and the cracking index. We will next examine the role the antishrinkage plays on these properties. The ultimate criterion for characterizing the packing density of a mixture at its final stage of elaboration is the packing index K [2,12], which is fixed at the value 7 for all the formulas, obviously excluding those for which the quantity of water is varied. For an average formula (550 kg of cement, equivalent granular proportions, 5 l of air), this index leads to a quantity of residual water per cubic meter about 20 l above the porosity of the packed solid skeleton under optimal conditions (packing index of 9). We use CPM to calculate the porosity. Under these conditions, if one varies the granular proportions or the cement dosage, the packing density of the mineral skeleton varies also and leads to a readjustment of the residual water. Inversely, when the quantity water is varied in an average formula of constant mineral skeleton, it is the level of packing that changes. The numerical values of these parameters are not given here. Only the curves showing the evolution of these parameters are presented in Fig. 5. In short:

(1) When the cement dosage (CEM I) varies from 350 to 700 kg/m^3 in the average formula:
- the quantity of water diminishes by 24 l,
- the compressive strength increases from 60 to 100 MPa for mixtures kept in cure and from 40 to 88 MPa for those kept in air,
- the total shrinkage passes from -650 to -900 10^{-6} for mixtures hardened in cure and from -1085 to -1200 10^{-6} for those kept in air right from their fabrication, with a minimum of -960 10^{-6} towards 450 kg of cement per cubic meter,
- the minimum cracking index is reached with mixtures kept in cure for 28 days. This change occurs for those hardened in air towards 550 kg of cement per cubic meter. Mixtures kept in cure for 160 days have a slightly higher index, between 2.5 and 2.6 depending on the cement dosage. Mixtures poor in cement kept in air have much higher index (3.3 for a cement dosage of 350 kg/m^3),
- a dosage of about 550 kg cement per cubic meter appears a good compromise to the risk of cracking for all modes of conservation.

(2) When the water dosage varies from 218 (minimal porosity of the solid packing minus entrapped air) to 298 l:
- the packing index diminishes from 9 to 4.6,
- the compressive strength diminishes from 92 to 66 MPa for mixtures hardened in cure and from 80 to 53 for those hardened in air,
- the total shrinkage passes from -660 to -1130 10^{-6} for mixtures hardened in cure and from -850 to -1670 10^{-6} for those kept in air right after their fabrication,
- the cracking index increases slightly, from around 2.25 to 2.6 for mixtures kept in air, from around 2.25 to 2.4 for those kept in cure for 28 days, and from 2.4 to 2.8 for those kept in cure for 160 days,
- the quantity of residual water therefore does not have a marked effect the cracking index. All the same, its dosage need be reduced to satisfy other properties (porosity, strength. . .).

(3) When the proportions of the sandstone sand Sg to the corrector sand Sc vary from 0 to 100% in the mixture:
- the quantity of water passes from 227 to 253 l/m^3,
- the compressive strength diminishes from 112 to 66 MPa for mixtures hardened in cure and from 92 to 57 for mixtures hardened in air,

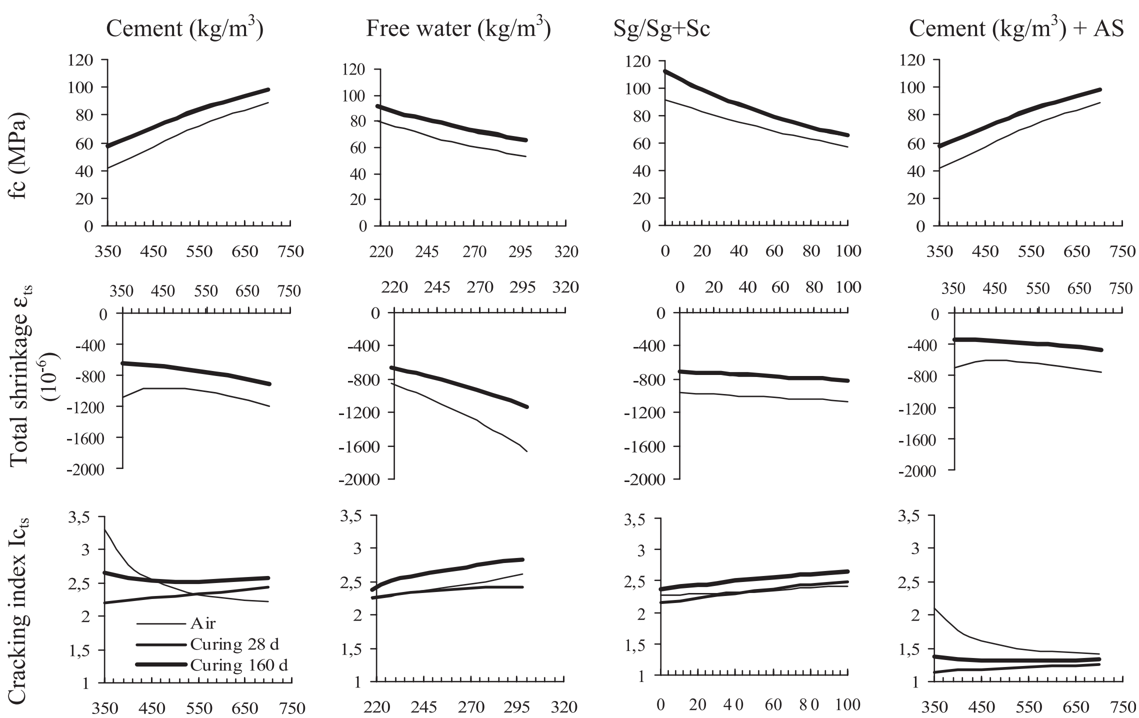

Fig. 5. Simulated properties on Day 1000.

- the total shrinkage passes from -710 to $-820\ 10^{-6}$ for mixtures hardened in cure and from -970 to $-1070\ 10^{-6}$ for those kept in air right after their fabrication,
- the cracking index increases from 2.27 to 2.43 for mixtures kept in air, from 2.15 to 2.5 for those kept in cure for 28 days, and from 2.4 to 2.5 for those kept in cure for 160 days,
- these behaviors are related to the difference in the granularity and in the morphological and mechanical properties (modulus) of the grains, which particularly influence the packing density and on the delayed modulus of the composite. To optimize the stability of the formula at the moment of casting, an equivalent dosage of two sands is recommended [12], which leads to the lowest the cracking index for mixtures that can be kept either in air or kept in cure for 28 days.

(4) Finally, the incorporation of a 2% cement weight of the antishrinkage admixture into the formulas significantly reduces the cracking index. Moreover, it is known that this admixture has a proved fluidizing effect, which is comparable to that of the organic product used [1]. For a cement dosage between 350 and 700 kg/m^3, one then obtains the same mechanical performances as before. On the contrary, the shrinkage reduces by 45%. The cracking index also diminishes significantly to the advantage of products kept in cure since the effectiveness of the product is better in these conditions (see the previous case). In the present case, the cracking index is between 1.14 and 1.26 for mixtures protected against air for 28 days.

In conclusion, according to the models, the proposed optimal formula for these artificial stones contains an equivalent mixture of two sands, a dosage in CEM I white cement of 550 kg/m^3, and a dose of 2% cement weight of the antishrinkage admixture. Addition of about 1 kg/m^3 of propylene polymer fibers provides extra security by homogenizing shrinkage cracks. The spin drying must be conducted in such way that every 1 m^3 of the fresh mixture retains about 240 l of water. The product must be kept in cure for more than 1 week and, if possible, for nearly 1 month. Its compressive strength will be of the order of 83 MPa, its long-term total shrinkage around 400 10^{-6}, and its cracking index will attain its maximum of 1.2 under relative hygrometry conditions of 50% HR. The final porosity of the stone will be around 17% and its medium-term carbonation rate will be low.

These models allow other simulations to be envisaged, especially concerning the presence of silica fumes and the duration of the curing. On an optimized formula, the adjusted models of the type AFREM or CEB-FIB allow the illustration of the role of the average radius of the pieces and of the ambient hygrometry (HR).

7. Conclusion

The work presented in this two-part article is on a coherent set of measurements realized on fine hydraulic mixtures known to be sensitive to shrinkages and on which little is published. A long analysis of the mass of measurements, collected between 100 and 800 days, allowed in the first place to find, with accuracy, the effective dosages of the sampled section cut horizontally from blocks presenting certain vertical variations in free water as well as the rates of hydration and carbonation of test pieces submitted to shrinkage tests. These two parameters explain certain behaviors observed. Mechanical performances measured in time showed that the strength model BetonlabPro2 software, based on a realistic consideration of the granular structure, the properties of the cement, aggregates, and additions, were valid for these products, with the exception of test pieces prematurely exposed to desiccation. An extension to this model was then proposed.

Similarly, the shrinkage models of this software, based on a theory of phase homogenization inside a three-sphere cell, globally reproduce observed dimensional variations. On the contrary, the predictions of more classical models dedicated to concrete shrinkages, such as those of CEB-FIB and of AFREM, deviate significantly from the observations. These discrepancies attributed to the different structure of these artificial stones with high porosity and sizeable strength. Adjustment of some of their coefficients allows the derivation of observed deformations in the range of formulas analyzed, characterized by lower endogenous shrinkage, and a higher total shrinkage than those of concretes containing coarse aggregates. We were able to determine a cracking index under conditions of inhibited shrinkage by comparing, in time and in the long term, the internal stress created by these deformations to the tensile strength of the products. In a general manner, this index exceeded the critical value, which is 1, as soon as the test pieces are exposed to desiccation for a few days with significant differences in the value depending on the terms of the formula and the duration of the cure. The simulations, however, showed that this risk could be reduced through a search for the most compact granular mixtures with a sufficient cement dosage and having just enough water to fill the porosity of the compact packing of the mineral skeleton. The method of fabrication adopted for these products allows in principle to realize these conditions by proceeding stage by stage. Finally, the use of propylene polymer fibers in association with an antishrinkage admixture leads to products of much better durability.

Acknowledgements

The authors are very grateful to Mr. Guy Feidt and Mr. Michel Pirotte of the company Société des Carrières Feidt (L) for their material and logistical support. They, in the same way, associate with this work, Mr Peter Strümper, a technician of the Luxemburg materials testing laboratory, who meticulously realized most of the measurements.

References

[1] A. Lecomte, N. Vulcano-Greullet, C. Steichen, G. Scharfe, Physical and mechanical properties of fine hydraulic mixtures, Cem. Conr. Res. 33 (2003) 1967–1981.

[2] Th. Sedran, F. de Larrard, BetonlabPro2, Logiciel de formulation des bétons, version 2.0 exécutable sous Windows, logiciel et notice, Presses de l'École nationale des Ponts et Chaussées, 2000.

[3] F. de Larrard, Concrete mixture proportioning, a scientific approach, Modern Concrete Technology, vol. 9, E&FN Spon, London, 1999.

[4] Final Draft of Eurocode 2: Design of concrete structures: Part 1. General rules and rules for buildings, 2001.

[5] R. Le Roy, F. de Larrard, G. Pons, Calcul des déformations instantanées et différées des BHP, Bull. Lab. Ponts Chaussées, spécial XIX (1996) 63–84.

[6] H.S. Müller, C.H. Küttner, V. Kvitsel, Creep and shrinkage models of normal and high-performance concrete—concept for a unified code-type approach, Creep and Shrinkage of Concrete, Special Issue of French Revue Of Genie Civil, Hermes, vol. 3–4, 1999, pp. 113–132.

[7] R. Le Roy, Déformations instantanées et différées des bétons à hautes performances, ER LCPC OA22, 1996.

[8] Z. Hashin, The elastic moduli of heterogeneous materials, J. Appl. Mech. 29 (1962) 143–150.

[9] Z. Hashin, S. Shtrikman, A variational approach o the theory of the elastic behavior of multiphase materials, J. Mech. Phys. Solids 11 (1963) 127–140.

[10] CEB-FIP Model Code 1990, CEB Bulletin d'Information, no. 213/214, Comité Euro-International du Béton - Fédération Internationale du Béton, Lausanne, Switzerland, 1993.

[11] P. Vezole, Recherche professionnelle relative aux bétons B25 et B40 avec fines d'addition, Annu. BTP 1 (2002) 31–43.

[12] A. Lecomte, N. Vulcano, Compactabilité de mélanges granulaires fins, Symp Physique et mécanique des matériaux granulaires, ENPC Paris, 2000, 327–332.